Front. Environ. Sci. Eng. 2018, 12(1): 8
https://doi.org/10.1007/s11783-018-1025-z

RESEARCH ARTICLE

Fe_2O_3-CeO_2-Bi_2O_3/γ-Al_2O_3 catalyst in the catalytic wet air oxidation (CWAO) of cationic red GTL under mild reaction conditions

Pan Gao[1], **Yuan Song**[1], **Shaoning Wang**[1], **Claude Descorme**[2], **Shaoxia Yang** (✉)[1]

1 National Engineering Laboratory for Biomass Power Generation Equipment, Beijing Key Laboratory of Energy Safety and Clean Utilization, School of Renewable Energy, North China Electric Power University, Beijing 102206, China
2 Institute for Research on Catalysis and Environment of Lyon (IRCELYON), UMR5256 CNRS –Claude Bernard Lyon 1 University, Albert Einstein Avenue, 69626, Villeurbanne, France

HIGHLIGHTS

- Fe_2O_3-CeO_2-Bi_2O_3/γ-Al_2O_3, an environmental friendly material, was investigated.
- The catalyst exhibited good catalytic performance in the CWAO of cationic red GTL.
- The apparent activation energy for the reaction was 79 $kJ \cdot mol^{-1}$.
- $HO_2\cdot$ and $O_2\cdot^-$ appeared as the main reactive species in the reaction.

ARTICLE INFO

Article history:
Received 22 September 2017
Revised 8 November 2017
Accepted 5 December 2017
Available online 18 January 2018

Keywords:
Catalytic wet air oxidation (CWAO)
Advanced oxidation processes (AOPs)
Iron oxide catalyst
Industrial wastewater

GRAPHIC ABSTRACT

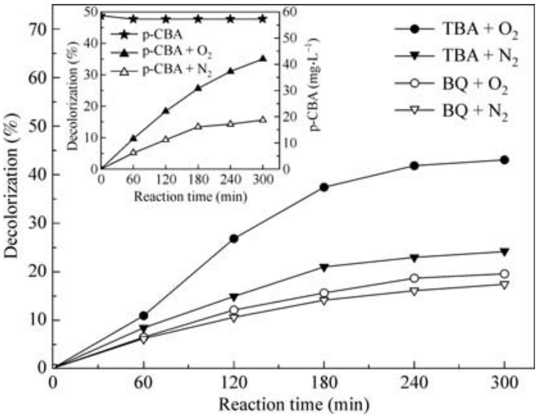

ABSTRACT

The Fe_2O_3-CeO_2-Bi_2O_3/γ-Al_2O_3 catalyst, a novel environmental-friendly material, was used to investigate the catalytic wet air oxidation (CWAO) of cationic red GTL under mild operating conditions in a batch reactor. The catalyst was prepared by wet impregnation, and characterized by special surface area (BET measurement), X-ray diffraction (XRD) and X-ray photoelectron spectroscopy (XPS). The Fe_2O_3-CeO_2-Bi_2O_3/γ-Al_2O_3 catalyst exhibited good catalytic activity and stability in the CWAO under atmosphere pressure. The effect of the reaction conditions (catalyst loading, degradation temperature, solution concentration and initial solution pH value) was studied. The result showed that the decolorization efficiency of cationic red GTL was improved with increasing the initial solution pH value and the degradation temperature. The apparent activation energy for the reaction was 79 $kJ \cdot mol^{-1}$. Hydroperoxy radicals ($HO_2\cdot$) and superoxide radicals ($O_2^-\cdot$) appeared as the main reactive species upon the CWAO of cationic red GTL.

1 Introduction

Industrial wastewaters, originating from the production of textiles, paper printing, plastics, rubber and medicines, often contain organic compounds with high concentration and toxicity. Such compounds could cause toxic effects on aquatic ecosystems and human health when directly discharged into water body. Biological treatments, the widest wastewater treatment technologies, are not appropriate for treating such wastewaters due to the bactericide properties of refractory compounds [1]. The development of effective technologies for removing pollutants has gained considerable attention. Advanced oxidation pro-

---

✉ Corresponding author
E-mail: yangshaoxia@ncepu.edu.cn

Special Issue—Advanced Treatment Technology for Industrial Wastewaters (Responsible Editors: Junfeng Niu & Hongbin Cao)

cesses (e.g. ozonation, photocatalysis, electrochemical oxidation) have shown good removal for refractory pollutants at a low concentration level [2–5].

Wet air oxidation (WAO) is one of effective technologies to deal with highly concentrated, toxic and hazardous organic compounds under high temperature (125–320°C) and pressure (0.5–20 MPa), and organic compounds were oxidized to CO_2, H_2O and innocuous compounds [6]. The WAO was commonly applied as a pretreatment process of the wastewaters before further using biological technologies [7]. The severely operating conditions to be implemented for the WAO reaction limit the practical application in the wastewater treatment. The catalysts added in the reaction, catalytic wet air oxidation (CWAO), can decrease the operating conditions, increase the oxidation rate and shorten the reaction time [8]. Compared with homogeneous catalysts, heterogeneous catalysts have shown good promise since they are easily separated from the effluents. Many heterogeneous catalysts have been developed in the CWAO of organic compounds, such as noble metal catalysts (Ru, Pt…) [9–12], transition metal oxides (CuO, Fe_2O_3, MnO_2…) [13–15] and carbon materials [16,17].

Especially, in the last decade some attempts have paid a lot attention to developing heterogeneous catalysts used under mild conditions, namely atmosphere pressure and low reaction temperature (< 100°C), in order to avoid the severely operating conditions in the CWAO reaction. For example, the catalysts (CuO-MoO_3-P_2O_5, $Zn_{1.5}PW_{12}O_{40}$, Mo-Zn-Al-O, $Pt/Ce_xZr_{1-x}O_2$…) exhibited good catalytic performance in the CWAO of different model compounds under atmospheric pressure [18–21]. It is noticed that active phases of these catalysts commonly contained high cost and free environmental-friendly metals. Therefore, the development of effective heterogeneous catalysts is a challenge in the CWAO under atmospheric pressure.

In the paper, a novel Fe_2O_3-CeO_2-Bi_2O_3/γ-Al_2O_3 catalyst was selected and developed. The reason are listed as follows: (1) iron oxide catalysts supported on γ-Al_2O_3, with high specific surface area and low cost, are the environmental-friendly materials and show good catalytic activity in the CWAO reactions because the electronic transformation of metal ions could produce strong oxidative species ($O_2^{-}\cdot$, $HO_2\cdot$…) [22,23]; (2) the oxygen vacancies on the CeO_2 surface are helpful to improve the formation of strong oxidative species [15,19]; (3) Ce and Bi not only exhibit good stability, but also have the catalytic performance in the CWAO reaction [24]. Cationic red GTL, widely used in the textile industry, was selected as a model molecule. The impact of the reaction conditions (catalyst loading, reaction temperature, solution concentration and initial solution pH) on the activity of the Fe_2O_3-CeO_2-Bi_2O_3/γ-Al_2O_3 catalyst was investigated in the CWAO of cationic red GTL under atmospheric pressure, and a mechanism of the catalyst was proposed.

2 Experimental

2.1 Materials

Cationic red GTL was supplied by Tianjin Fuchen Fine Chemical Plant (China). Its chemical structure was shown in the literature [20], and its pK_a was ca. 4.7 measured by the literature [25]. Other reagents used for the different experiments were all of analytical grade. γ-Al_2O_3 was purchased from Aladdin Industrial Corporation and used as a support. The powder size was ca. 100 μm.

2.2 Catalyst preparation

The catalyst was synthesized by wet impregnation method. First, $Bi(NO_3)_3\cdot 5H_2O$ was dissolved in the dilute nitric acid, and then $Fe(NO_3)_3\cdot 9H_2O$ and $Ce(NO_3)_3\cdot 6H_2O$ were added into the solution under vigorous stirring. Secondly, γ-Al_2O_3 support was loaded above the mixed solution, kept under sonication for 15 min (250 W, 40 kHz), and then impregnated at room temperature overnight. The resulting mixture was dried at 110°C overnight and calcined at 400°C for 3 h under flowing air (400 $mL\cdot min^{-1}$) to get the Fe_2O_3-CeO_2-Bi_2O_3/γ-Al_2O_3 catalyst. The corresponding Fe_2O_3/γ-Al_2O_3 and Fe_2O_3-CeO_2/γ-Al_2O_3 catalysts were prepared following a similar process. Fe, Ce and Bi loadings on the γ-Al_2O_3 were ca. 3.5, 2.4 and 1.8 wt.% for all catalysts, respectively.

2.3 Catalyst characterization

The specific surface area of the samples was measured by N_2 adsorption at 77 K using an analyzer (Autosorb IQ-MP, USA). Before the analysis, the samples were outgassed at 250°C for 4 h. X-ray diffraction (XRD) analysis was carried out on a diffractometer (Bruker D8 advance, Germany) in the range 20°–80° using a Cu K_a radiation source ($\lambda = 0.15406$ nm) and a scanning speed of $4°\cdot min^{-1}$. X-ray photoelectron spectroscopy (XPS) study was performed on an analyzer (PHI 5400 ESCA, USA) using an Al K_a X-ray source ($h\nu = 1486.60$ eV). The C1s peak ($E_b = 284.60$ eV), originating from the surface contamination, was used as a reference for the calibration of the binding energies. The pH at the point of zero charge (pH_{PZC}) of different materials was measured with the method developed by Noh et al. [26].

2.4 CWAO reaction

All experiments were performed in a glass reactor. It was kept into a water bath in order to maintain the stable reaction temperature during the experiments, and equipped with a magnetic stirrer to ensure good mass transformation. 250 mL cationic red GTL solution (100 $mg\cdot L^{-1}$, $pH_0 = 5.4$)

was loaded into the reactor, while pure O_2 (200 mL·min^{-1}) was continuously bubbled into the solution with stirring. After heating the reactor up to the desired temperature, a fixed amount catalyst was introduced into the reactor, and this time was defined as the "zero" time. In parallel, in order to evaluate the adsorption capacity of the catalyst, the same experiment was performed under N_2 bubbling. Upon the reaction, the samples were periodically withdrawn from the reactor. After being filtrated with a 0.22 μm filter to eliminate any solid catalyst particles, the liquid samples were analyzed with a UV-vis spectrophotometer and measured at 530 nm. The evaluation of the catalytic activity was based on the measurement of the decolorization efficiency (%) and calculated as follows:

$$\text{Decolorization } = \frac{c_0 - c_t}{c_0} \times 100, \tag{1}$$

where c_0 and c_t were the initial and final concentration of cationic red GTL in the reaction, respectively. The intermediates produced during the CWAO reaction were analyzed by high performance liquid chromatogram (HPLC) with a UV detector using a C18 column. The mobile phase was a mixture of 0.09% phosphoric acid aqueous solution and methane (v/v, 90:10) with a flow rate of 1.0 mL·min^{-1}. The effluents in the reaction were further analyzed by ICP to check any possible leaching of Fe, Ce, Bi and Al from the catalyst.

3 Results and discussion

3.1 Characterization of the catalyst

3.1.1 BET and pH$_{\mathrm{PZC}}$

The specific surface areas of the samples were summarized in Table 1. γ-Al_2O_3 had a pretty large specific surface area (ca. 166 m^2·g^{-1}). Compared with that of the support, the specific surface areas of the catalysts (Fe_2O_3/γ-Al_2O_3, Fe_2O_3-CeO_2/γ-Al_2O_3 and Fe_2O_3-CeO_2-Bi_2O_3/γ-Al_2O_3) slightly decreased, indicating that the impregnation of the active components did not significantly affect the accessibility of the porous structure of the support.

The pH$_{\mathrm{PZC}}$ of the samples was close to 8.0, while the pH$_{\mathrm{PZC}}$ of the catalysts slightly decreased compared to that of the support (pH$_{\mathrm{PZC}}$ = 8.22). Such differences could potentially alter the catalysts surface charge upon reaction and subsequently affect the dye adsorption on the catalyst surface [27]. The charge on the catalyst surface would be positive below the solution of 8.0 pH value, and on the contrary the charge on the catalyst surface would be negative.

3.1.2 XRD

The XRD patterns of the samples were shown in Fig. 1. The support was characterized by three main typical diffraction lines at 37.6°, 45.9° and 67.0°. These peaks were also observed for all catalysts and the intensity of the peaks did not obviously change, indicating that active phases supported on γ-Al_2O_3 did not affect the crystalline structure of the support. In addition, very weak and broad diffraction peaks at ca. 32.8° and 53.8°, attributed to α-Fe_2O_3, were observed in the XRD pattern of Fe_2O_3/γ-Al_2O_3 catalyst, indicating that Fe_2O_3 particles with very small crystal size were well-dispersed on the support. When Ce and Bi were impregnated on the support, the relative Fe diffraction peaks disappeared from the XRD patterns. The observation indicated that the addition of Ce and Bi promoted the dispersion of Fe_2O_3 particles. No relative Ce and Bi diffraction peaks were observed on the XRD patterns, probably because of low loadings of Ce and Bi.

3.1.3 XPS

The surface composition and the element chemical state of the samples were determined with XPS, and the spectra for Fe, Ce and Bi were shown in Fig. 2 in the case of the Fe_2O_3-CeO_2-Bi_2O_3/γ-Al_2O_3 catalyst. The XPS spectra of Ce 3d and Bi 4f were observed, and assigned to CeO_2 and Bi_2O_3, in agreement with the preparation process of the catalysts. By comparison with the spectra obtained for Fe_2O_3/Al_2O_3 and Fe_2O_3-CeO_2/γ-Al_2O_3 catalysts, it is observed that the binding energy of Fe 2p$_{3/2}$ was slightly shifted toward lower binding energy upon the addition of Ce and Bi, indicating a change in the chemical state of Fe. To get deeper insights into the change, the Fe 2p$_{3/2}$ spectra were fitted with two bands, i.e. a main peak ca. 711.0 eV attributed to Fe^{3+}-O and a smaller peak ca. 709.5 eV assigned to Fe^{2+}-O [28,29]. The amounts of Fe^{2+} increased and were 5.43 , 8.74 and 11.09 at.% for Fe_2O_3/γ-Al_2O_3, Fe_2O_3-CeO_2/γ-Al_2O_3 and Fe_2O_3-CeO_2-Bi_2O_3/γ-Al_2O_3 catalysts, respectively (in Table 1). In addition, Al and O spectra were obtained for different catalysts. No obvious

Table 1 The structure of the catalysts

Samples	Surface area (m^2·g^{-1})	pH$_{\mathrm{PZC}}$	Fe^{2+} (at.%)	Fe^{3} (at.%)	Loading of metals (wt.%)		
					Fe	Ce	Bi
Fe_2O_3/γ-Al_2O_3	163	7.64	5.43	94.57	3.51	–	–
Fe_2O_3-CeO_2/γ-Al_2O_3	160	7.78	8.74	91.26	3.49	2.41	–
Fe_2O_3-CeO_2-Bi_2O_3/γ-Al_2O_3	157	7.94	11.09	88.91	3.47	2.38	1.82

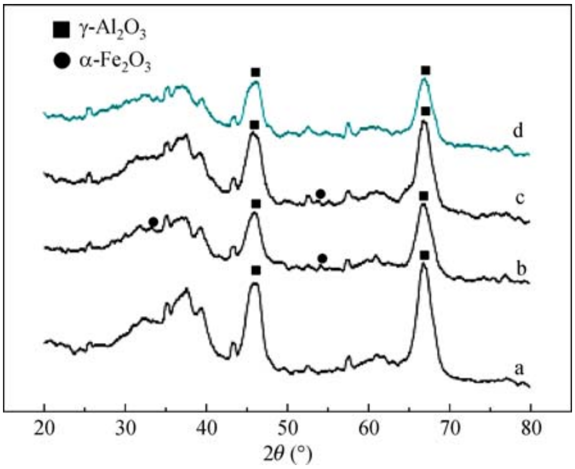

Fig. 1 XRD patterns of the support and catalysts (a: γ-Al_2O_3, b: Fe_2O_3/γ-Al_2O_3, c: Fe_2O_3-CeO_2/γ-Al_2O_3, d: Fe_2O_3-CeO_2-Bi_2O_3/γ-Al_2O_3)

change in the Al XPS spectra was observed for all catalysts (see Fig. S1 in Supplementary material). A slight shift forward high binding energy for the O 1s spectra was observed for the different catalysts (see Fig. S2 in Supplementary material), when Ce and Bi were added to the Fe_2O_3/γ-Al_2O_3 catalyst.

3.2 CWAO of cationic red GTL

CWAO of cationic red GTL was studied under various conditions, including stirring speed, oxygen flow rate, catalyst loading, catalyst type, initial solution pH, reaction temperature, and initial concentration of cationic red GTL.

The O_2 partial pressure has some impact on the conversion of pollutants in the CWAO reaction [9,10,19]. In our experiments, the effect of the stirring speed and oxygen flow rate was measured in order to eliminate any possible oxygen transformation limitations and ensure the performance of the catalysts under chemical control. Under the applied reaction conditions, the decolorization efficiency was observed to be constant when the stirring speed and oxygen flow rate were over 650 r·min^{-1} and 200 mL·min^{-1}, respectively.

The effect of the catalyst loading (1, 2, 3 and 4 g·L^{-1}) on the decolorization efficiency of the dye was evaluated at 70°C under atmospheric pressure. The reaction rate was expressed per gram of a catalyst. The reaction rate rapidly increased from 1 to 2 g·L^{-1} catalyst loading; however it decreased at the higher catalyst loading. The catalyst loading was fixed at 2 g·L^{-1} in the following experiments to make sure that the reaction was performed under kinetic control.

3.2.1 Impact of the different catalysts

Upon the WAO of cationic red GTL without any catalysts (in Fig. 3), the decolorization efficiency was almost zero after 240 min reaction at 70°C under O_2 bubbling. In conclusion, cationic red GTL was shown to be stable under our operating conditions. Under N_2 bubbling, the adsorption of cationic red GTL on the different catalysts was assessed under the same reaction conditions. It is found that a fraction of cationic red GTL was adsorbed on the catalysts (up to 20%). Indeed, the high dye adsorption on the catalysts would be attributed to the specific surface area of the catalysts (ca. 160 m^2·g^{-1}). Under O_2 bubbling, the support was shown to be totally inactive. On the opposite, the different catalysts exhibited the decolorization performances. After 240 min reaction at 70°C, the decolorization reached 32, 38 and 46% over the Fe_2O_3/γ-Al_2O_3, Fe_2O_3-CeO_2/γ-Al_2O_3 and Fe_2O_3-CeO_2-Bi_2O_3/γ-Al_2O_3 catalysts, respectively. The decolorization of the solution should be attributed to the combined effects of the adsorption and the activity of the catalysts. Moreover, the addition of Ce and Bi improved the activity of the Fe_2O_3/γ-Al_2O_3 catalyst. No leaching of Fe, Ce, Bi and Al was detected upon completion of the reaction, indicating that the iron oxides-based catalysts were active and stable under the applied reaction conditions. The main intermediates, as identified by HPLC, were hydroquinone and 1-chloro-3-nitro-benzene.

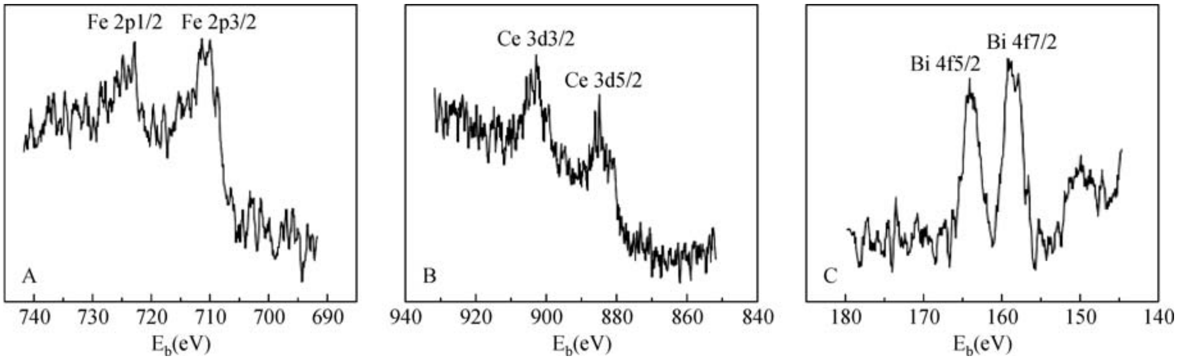

Fig. 2 XPS spectra of Fe_2O_3-CeO_2-Bi_2O_3/γ-Al_2O_3 catalyst

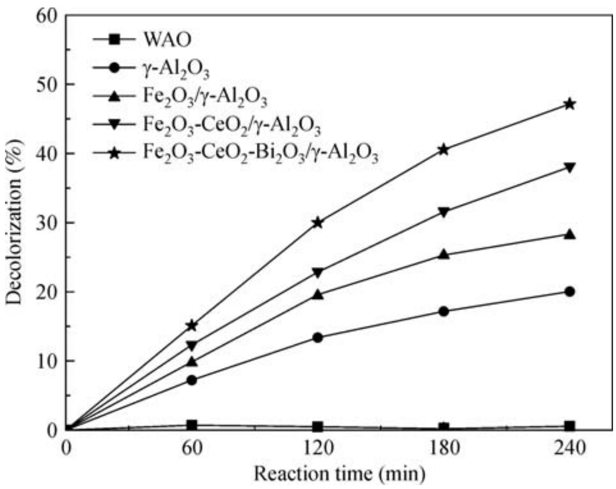

Fig. 3 Decolorization efficiency of cationic red GTL in CWAO over the different catalysts under atmospheric pressure ($[Dye]_0$= 100 $mg \cdot L^{-1}$; $[Catalyst]_0$ = 2.0 $g \cdot L^{-1}$; $[O_2]_0$= 200 $mL \cdot min^{-1}$; T= 70 °C)

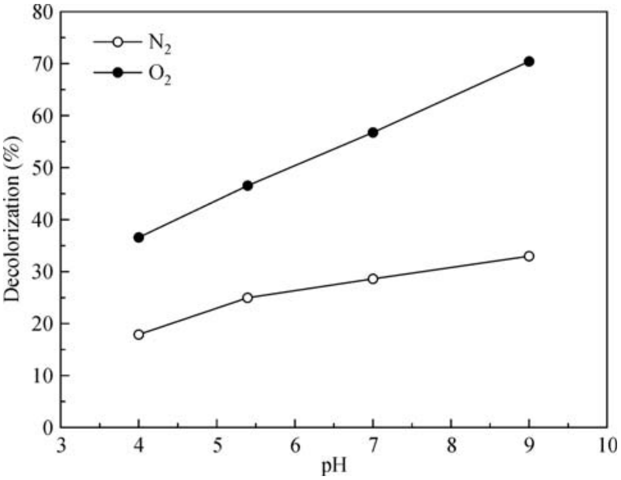

Fig. 4 Effect of initial pH value of cationic red GTL solution on the decolorization efficiency in the CWAO over the Fe_2O_3-CeO_2-Bi_2O_3/γ-Al_2O_3 catalyst under atmospheric pressure ($[Dye]_0$= 100 $mg \cdot L^{-1}$; $[Catalyst]_0$= 2.0 $g \cdot L^{-1}$; $[O_2]_0$= 200 $mL \cdot min^{-1}$; T= 70 °C)

3.2.2 Impact of initial solution pH

Figure 4 showed the effect of initial pH of the cationic red GTL solution (4.0, 7.0 and 9.0) on the decolorization of cationic red GTL upon the CWAO over Fe_2O_3-CeO_2-Bi_2O_3/γ-Al_2O_3 catalyst at 70°C under atmospheric pressure. Upon increase of initial pH of the solution under N_2 bubbling (adsorption), the decolorization increased from 18 to 30% after 240 min reaction. Similarly, under O_2 bubbling, the decolorization was enhanced from 33 to 67%. The adsorption of cationic red GTL on the solid surface was affected by the pH of the solution, especially with respect to the pK_a of cationic red GTL (4.7) and the pH_{pzc} of the solid (ca. 8). Indeed, upon the CWAO of cationic red GTL, the different situations might be encountered: (1) when initial pH value of the solution was acidic (4.0), i.e below the pH_{pzc} of the catalyst and the pK_a of cationic red GTL, the catalyst surface will be positively charged and the dye will be in the cationic form; resulting in repulsive electrostatic interactions between the cationic dye and the positively charged surface of the catalyst, preventing the adsorption of the dye on the catalyst and inhibiting the reaction of the the dye on the catalyst surface; (2) when initial pH of the solution was above 4.7 (7.0 and 9.0), i.e above the pK_a of cationic red GTL, the dye will exist in the molecular form and non-specific weak interactions with the catalyst surface will occur, leading to the adsorption and the further reaction of cationic red GTL at the catalyst surface. Therefore, the adsorption appeared to be a key parameter controlling the catalytic performance of the Fe_2O_3-CeO_2-Bi_2O_3/γ-Al_2O_3 catalyst in the CWAO of cationic red GTL.

3.2.3 Impact of the degradation temperature

The effect of the reaction temperatures (70°C, 80°C and 90°C) on the activity of the Fe_2O_3-CeO_2-Bi_2O_3/γ-Al_2O_3 catalyst was investigated in the CWAO of cationic red GTL under atmospheric pressure (in Fig. 5). With increasing reaction temperature, the decolorization removal increased from 18 up to 76% after 240 min reaction, and the initial reaction rate (attributed to the activity of the catalyst) increased from 1.7, 3.2 to 8.4 $mg_{GTL} \cdot g_{cat}^{-1} \cdot h^{-1}$, respectively. According to the Arrhenius plot, the apparent activation energy was calculated to be ca. 79 $kJ \cdot mol^{-1}$ in the CWAO of cationic red GTL over the Fe_2O_3-CeO_2-Bi_2O_3/γ-Al_2O_3 catalyst. The relative literatures did not involve the activation energy in the CWAO of the cationic ion red GTL, so no comparison was possible.

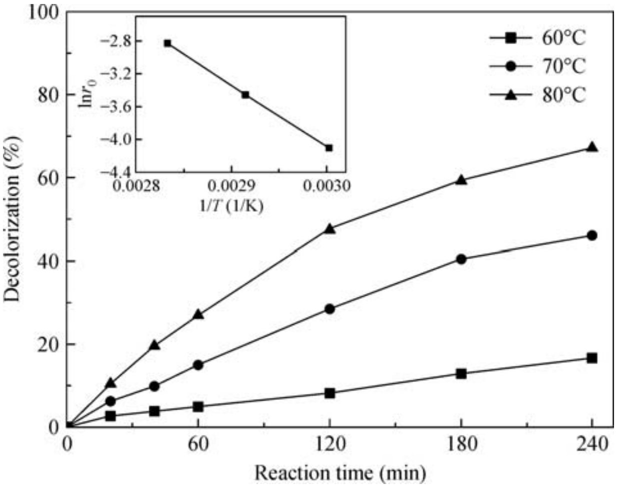

Fig. 5 Effect of reaction temperature on the decolorization efficiency of cationic red GTL in the CWAO over the Fe_2O_3-CeO_2-Bi_2O_3/γ-Al_2O_3 catalyst under atmospheric pressure ($[Dye]_0$= 100 $mg \cdot L^{-1}$; $[Catalyst]_0$= 2.0 $g \cdot L^{-1}$; $[O_2]_0$= 200 $mL \cdot min^{-1}$)

3.2.4 Impact of the solution concentration

The effect of the cationic ion red GTL concentration (50, 100 and 150 mg·L^{-1}) on the activity of the Fe_2O_3-CeO_2-Bi_2O_3/γ-Al_2O_3 catalyst was investigated at 70°C under atmosphere pressure (in Fig. 6). With increasing the solution concentration, the decolorization removal decreased, and the initial reaction rates (attributed to the activity of the catalyst) were 1.8, 3.2 and 3.5 $mg_{GTL}\cdot g_{cat}^{-1}\cdot h^{-1}$, respectively. A reaction order with respect to cationic ion red GTL concentration was ca. 0.6 under the applied reaction conditions. This indicates that the initial reaction rate has a close connection with the concentration of cationic ion red GTL.

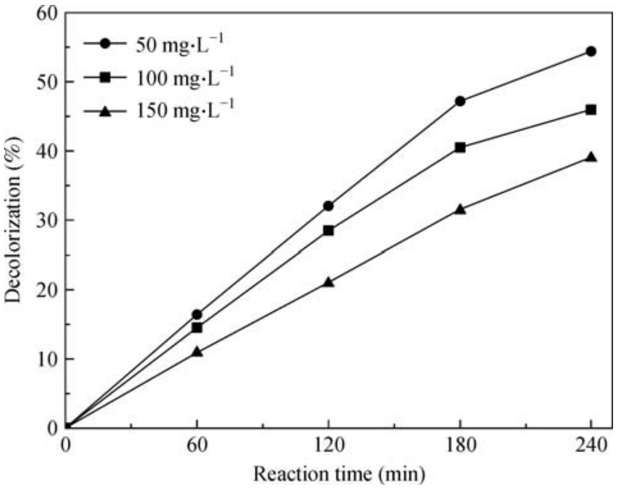

Fig. 6 Effect of the cationic red GTL concentration on the decolorization efficiency in the CWAO over the Fe_2O_3-CeO_2-Bi_2O_3/γ-Al_2O_3 catalyst under atmosphere pressure ($[Catalyst]_0$= 2.0 g·L^{-1}, $[O_2]_0$= 200 mL·min^{-1}, T= 70 °C)

3.3 Insight into the reaction mechanism

While it is well accepted in the literatures that the CWAO of organic compounds involves a free radical mechanism, the nature of strong oxidative species formed in the process (e.g. $O_2^-\cdot$, $HO_2\cdot$, $OH\cdot$) is still a question of debate due to the severely operating conditions [10,16,30]. To detect active species formed in the CWAO of cationic red GTL over the Fe_2O_3-CeO_2-Bi_2O_3/γ-Al_2O_3 catalyst under mild conditions, a series of experiments were performed in the presence of different radical scavengers. Tert-butyl alcohol (TBA) and p-benzoquinone (BQ) were used as scavengers for $OH\cdot$ and $HO_2\cdot/O_2^-\cdot$ radicals, respectively. In addition, para-chlorobenzoic acid (*p*-CBA) was also used as an indicator to detect the presence of $OH\cdot$ radicals upon the CWAO of cationic red GTL, since it would be only oxidized by $OH\cdot$ radicals [31,32].

Looking at the possible involvement of radicals, the experiments were performed in the presence p-CBA, TBA and BQ, respectively. As shown in Fig. 7, it is found after 240 min reaction that: (1) the presence of BQ induced a decrease of the decolorization efficiency from 45 to 22%; (2) the decolorization removal of cationic red GTL did not almost change in the presence of TBA; (3) *p*-CBA did not be oxidized upon the CWAO. The result clearly demonstrated that $OH\cdot$ radicals were not generated and $O_2^-\cdot$/$HO_2\cdot$ radicals were the main oxygen species in the CWAO of cationic red GTL over the Fe_2O_3-CeO_2-Bi_2O_3/γ-Al_2O_3 catalyst.

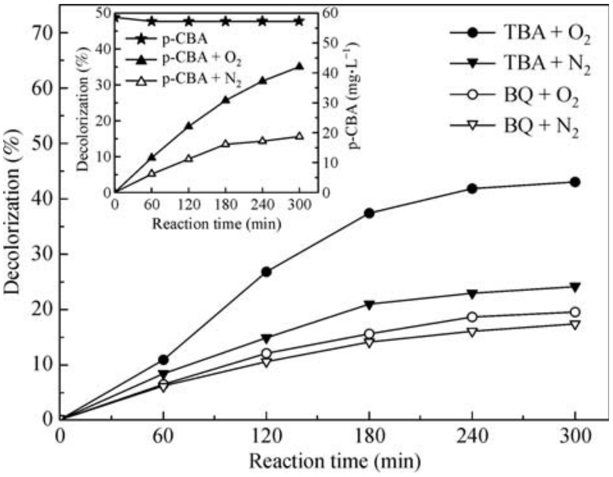

Fig. 7 Effect of scavenging agents on the decolorization efficiency of cationic red GTL in the CWAO over Fe_2O_3-CeO_2-Bi_2O_3/γ-Al_2O_3 catalyst under atmospheric pressure ($[Dye]_0$= 100 mg·L^{-1}; $[Catalyst]_0$= 2.0 g·L^{-1}; $[O_2]_0$= 200 mL·min^{-1}; T= 70 °C)

In the CWAO of cationic red GTL, O_2 would first adsorb on the catalyst surface and trap an electron from iron (Fe^{2+}) to produce $O_2^-\cdot$, and then further react with protons to form $HO_2\cdot$ in the solution. Both radicals would be responsible for the oxidation of cationic red GTL. The activity of the iron catalysts could be related to the fraction of Fe^{2+} in the catalyst that might be oxidized upon the adsorption of oxygen, alone with the production of $O_2^-\cdot$/$HO_2\cdot$ radicals. Therefore, the structural properties of the Fe_2O_3-CeO_2-Bi_2O_3/γ-Al_2O_3 catalyst (high specific surface area, pH_{PZC} and high amount of Fe^{2+}) would be responsible for the efficient production of $O_2^-\cdot/HO_2\cdot$ radicals, and lead to good catalytic activity for the CWAO of cationic red GTL.

We compared with the initial reaction rate of the Fe_2O_3-CeO_2-Bi_2O_3/γ-Al_2O_3 and Mo-Zn-Al-O catalysts in the CWAO of cationic red GTL under atmosphere pressure [20]. For the Fe_2O_3-CeO_2-Bi_2O_3/γ-Al_2O_3 catalyst, the initial reaction rate, expressed per gram of active phases of Fe, Ce and Bi, was ca. 49 $mg_{GTL}\cdot g_{metals}^{-1}\cdot h^{-1}$ at 70°C, while the initial reaction rate for the Mo-Zn-Al-O catalyst was ca. 28 $mg_{GTL}\cdot g_{metals}^{-1}\cdot h^{-1}$ at room temperature. The result indicates that the environmental-friendly Fe_2O_3-

CeO_2-Bi_2O_3/γ-Al_2O_3 catalyst with low cost has the application potential in the wastewater treatment.

4 Conclusions

Iron oxide-supported catalysts, the environmental-friendly materials, were investigated in the CWAO of cationic red GTL under atmospheric pressure. The Fe_2O_3-CeO_2-Bi_2O_3/γ-Al_2O_3 catalyst showed good decolorization efficiency, which was enhanced by the addition of Ce and Bi. Indeed, the addition of Ce and Bi improved the iron dispersion and increased the fraction of Fe^{2+} in the catalyst. The decolorization efficiency was enhanced when the adsorption of cationic red GTL on the catalyst surface could be promoted upon CWAO reaction. Superoxide and hydroperoxyl radicals were identified as the main reactive oxidative species in the CWAO of cationic red GTL over the Fe_2O_3-CeO_2-Bi_2O_3/γ-Al_2O_3 catalyst.

Acknowledgements This work was supported by the National Natural Science Foundation of China (Grant Nos. 21547008 & 51206045), School featured projects (No. TS2016HBDL16) and Fundamental Research Funds for Central Universities (No. 2015 MS21).

Electronic Supplementary Material Supplementary material is available in the online version of this article at https://doi.org/10.1007/s11783-018-1025-z and is accessible for authorized users.

References

1. Sang H L, Carberry J B. Biodegradation of PCP enhanced by chemical oxidation pretreatment. Water Environment Research, 1992, 64(5): 682–690
2. Tian S C, Li Y B, Zhao X. Cyanide removal with a copper/active carbon fiber cathode via a combined oxidation of a Fenton-like reaction and *in situ* generated copper oxides at anode. Electrochimica Acta, 2015, 180: 746–755
3. Liao G, Zhu D, Li L, Lan B. Enhanced photocatalytic ozonation of organics by g-C_3N_4 under visible light irradiation. Journal of Hazardous Materials, 2014, 280: 531–535
4. Wang Y B, Zhao H, Zhao G. Iron-copper bimetallic nanoparticles embedded within ordered mesoporous carbon as effective and stable heterogeneous Fenton catalyst for the degradation of organic contaminants. Applied Catalysis B: Environmental, 2015, 164: 396–406
5. Xiao J D, Xie Y B, Nawaz F, Jin S, Duan F, Li M J, Cao H B. Super synergy between photocatalysis and ozonation using bulk g-C_3N_4 as catalyst: A potential sunlight/O_3/g-C_3N_4 method for efficient water decontamination. Applied Catalysis B: Environmental, 2016, 181: 420–428
6. Luck F. Wet air oxidation: Past, present and future. Catalysis Today, 1999, 53(1): 81–91
7. Kim K H, Ihm S K. Heterogeneous catalytic wet air oxidation of refractory organic pollutants in industrial wastewaters: A review. Journal of Hazardous Materials, 2011, 186(1): 16–34
8. Mezohegyi G, Erjavec B, Kaplan R, Pintar A. Removal of bisphenol A and its oxidation products from aqueous solutions by sequential catalytic wet air oxidation and biodegradation. Industrial & Engineering Chemistry Research, 2013, 52(26): 9301–9307
9. Wang J B, Zhu W P, Yang S X, Wang W, Zhou Y R. Catalytic wet air oxidation of phenol with pelletized ruthenium catalysts. Applied Catalysis B: Environmental, 2008, 78(1–2): 30–37
10. Yang S X, Besson M, Descorme C. Catalytic wet air oxidation of succinic acid over Ru and Pt catalysts supported on $Ce_xZr_{1-x}O_2$ mixed oxides. Applied Catalysis B: Environmental, 2015, 165 (165): 1–9
11. De los Monteros A E, Lafaye G, Cervantes A, Del Angel G, Barbier JJr. Catalytic wet air oxidation of phenol over metal catalyst (Ru, Pt) supported on TiO_2-CeO_2 oxides. Catalysis Today, 2015, 258: 564–569
12. Szabados E, Sagi G, Somodi F, Maroti B, Sranko D, Tungler A. Wet air oxidation of paracetamol over precious metal/Ti mesh monolith catalyst. Journal of Industrial and Engineering Chemistry, 2017, 46: 364–372
13. Xu A, Sun C. Catalytic behaviour and copper leaching of $Cu_{0.10}Zn_{0.90}Al_{1.90}Fe_{0.10}O_4$ spinel for catalytic wet air oxidation of phenol. Environmental Technology, 2012, 33(10–12): 1339–1344
14. Ersöz G, Atalay S. Treatment of aniline by catalytic wet air oxidation: Comparative study over CuO/CeO_2 and NiO/Al_2O_3. Journal of Environmental Management, 2012, 113(4): 244–250
15. Ma C J, Wen Y Y, Yue Q Q, Li A Q, Fu J L, Zhang N, Gai H, Zheng J, Chen B H. Oxygen-vacancy-promoted catalytic wet air oxidation of phenol from MnO_x-CeO_2. RSC Advances, 2017, 7 (43): 27079–27088
16. Rocha R P, Silva A M T, Romero S M M, Pereira M F R, Figueiredo J L. The role of O- and S-containing surface groups on carbon nanotubes for the elimination of organic pollutants by catalytic wet air oxidation. Applied Catalysis B: Environmental, 2014, 147(14): 314–321
17. Yang S, Cui Y, Sun Y, Yang H. Graphene oxide as an effective catalyst for wet air oxidation of phenol. Journal of Hazardous Materials, 2014, 280: 55–62
18. Ma H, Zhuo Q, Wang B. Characteristics of CuO-MoO_3-P_2O_5 catalyst and its catalytic wet oxidation (CWO) of dye wastewater under extremely mild conditions. Environmental Science & Technology, 2007, 41(21): 7491–7496
19. Yang S X, Besson M, Descorme C. Catalytic wet air oxidation of formic acid over $Pt/Ce_xZr_{1-x}O_2$ catalysts at low temperature and atmospheric pressure. Applied Catalysis B: Environmental, 2010, 100(1–2): 282–288
20. Xu Y, Li X, Cheng X, Sun D, Wang X. Degradation of cationic red GTL by catalytic wet air oxidation over Mo-Zn-Al-O catalyst under room temperature and atmospheric pressure. Environmental Science & Technology, 2012, 46(5): 2856–2863
21. Zou L, Wang Q, Wang Z, Jin L, Liu R J, Shen X Q. Rapid decolorization of methyl blue in aqueous solution by recyclable microchannel-like $La_{0.8}K_{0.2}FeO_3$ hollow microfibers. Industrial & Engineering Chemistry Research, 2013, 53(2): 658–663
22. Quintanilla A, Casas J A, Rodríguez J J. Catalytic wet air oxidation of phenol with modified activated carbons and Fe/activated carbon

catalysts. Applied Catalysis B: Environmental, 2007, 76(1–2): 135–145

23. di Luca C, Ivorra F, Massa P, Fenoglio R. Iron-alumina synergy in the heterogeneous Fenton-type peroxidation of phenol solutions. Chemical Engineering Journal, 2015, 268: 280–289
24. Zhu W, Bin Y, Li Z, Jiang Z, Yin T. Application of catalytic wet air oxidation for the treatment of H-acid manufacturing process wastewater. Water Research, 2002, 36(8): 1947–1954
25. Wang X M, Waite T D. Role of gelling soluble and colloidal microbial products in membrane fouling. Environmental Science & Technology, 2009, 43(24): 9341–9347
26. Noh J S, Schwarz J A. Effect of HNO_3 treatment on the surface acidity of activated carbons. Carbon, 1990, 28(5): 675–682
27. Karpel N, Leitner V, Fu H X. pH effects on catalytic ozonation of carboxylic acids with metal on metal oxides catalysts. Topics in Catalysis, 2005, 33(1–4): 249–256
28. Descostes M, Mercier F, Thromat N, Beaucaire C, Gautier-Soyer M. Use of XPS in the determination of chemical environment and oxidation state of iron and sulfur samples: Constitution of a data basis in binding energies for Fe and S reference compounds and applications to the evidence of surface species of an oxidized pyrite in a carbonate medium. Applied Surface Science, 2000, 165(4): 288–302
29. Guo L Q, Chen F, Fan X Q, Cai W D, Zhang J L. S-doped α-Fe_2O_3 as a highly active heterogeneous Fenton-like catalyst toward the degradation of acid orange 7 and phenol. Applied Catalysis B: Environmental, 2010, 96(1–2): 162–168
30. Barbier JJr, Delanoë F, Jabouille F, Duprez D, Blanchard G, Isnard P. Total oxidation of acetic acid in aqueous solutions over noble metal catalysts. Journal of Catalysis, 1998, 177(2): 378–385
31. Rosenfeldt E J, Linden K G, Canonica S, von Gunten U. Comparison of the efficiency of $^{\cdot}$OH radical formation during ozonation and the advanced oxidation processes O_3/H_2O_2 and UV/H_2O_2. Water Research, 2006, 40(20): 3695–3704
32. Yang Y, Jiang J, Lu X, Ma J, Liu Y. Production of sulfate radical and hydroxyl radical by reaction of ozone with peroxymonosulfate: A novel advanced oxidation process. Environmental Science & Technology, 2015, 49(12): 7330–7339